EFFECT OF STAND-OFF DISTANCE ON THE MICROSTRUCTURAL, MECHANICAL AND PHYSICAL PROPERTIES OF Al-Zn PSEUDO-ALLOY COATING PREPARED VIA WIRE ARC SPRAY PROCESS

Nur Suhaili Ismail**,** Nor Akmal Fadil and Tuty Asma Abu Bakar*

[1]School of Mechanical Engineering, Faculty of Engineering, Universiti Teknologi Malaysia, 81310, Johor Bahru, Johor, Malaysia

*tuty@utm.my

Abstract. Protective coating has been one of the most effective corrosion mitigation methods. Therefore, it has been utilized to protect steel substrates for decades. Among various coating techniques, the twin wire arc spray (TWAS) process has been widely adopted in surface engineering to protect components due to its cost efficiency and flexibility. It promotes superior coating quality: low porosity, high hardness, and high adhesion. However, it is crucial to set the proper coating process parameters as coating properties produced via TWAS usually have high roughness and low adhesion to substrates. In this study, two different wires feedstock of Al and Zn were used to produce a pseudo-alloy of Al-50Zn alloy coating on mild steel substrates. In this research, the stand-off distance (SOD) parameter was varied at 100, 150, 200, 250, and 300 mm. The effect on the properties of developed coating layer on microstructure, thickness, hardness, roughness, and adhesion was investigated. The microstructure and morphological analyses were conducted using SEM and the phase analysis using XRD. Results have shown that the samples prepared at 100 mm have demonstrated the best coating quality compared to others and there are pronounced correlations between process parameters and all coating properties. The average thickness of the coating at 100 mm SOD was recorded to be the lowest at 230 μm with the highest hardness and adhesion values, 109 Hv and 8.3 MPa, respectively and the lowest surface roughness of 5.1 microns. Contrasts with coating prepared at 300 mm SOD that has demonstrated poor qualities in both microstructural and mechanical properties.

Keywords: thermal spray process, wire arc spray, pseudo alloy; aluminium alloy, corrosion protection

Article Info

Received 30th December 2021
Accepted 4th April 2022
Published 20th April 2022

ISSN: 1823-7010, eISSN: 2600-7444

Introduction

Mild steel, known for its excellent mechanical properties, availability, machinability, low cost has been widely used in essential fields such as oil and gas industries, pipelines, power plants, and food processing industries. However, these advantages come with some significant drawbacks; it suffers corrosion at a high rate in its original form, especially in harsh environments such as chloride or high temperature. Thus, protective coating is critical for mild steel to function effectively in such conditions for a long period. Many protective coating methods exist, such as hot-dip, physical vapour deposition (PVD), chemical vapour deposition (CVD), and various thermal spray methods. Research has shown that the thermal spray process promotes superior coating qualities; good adhesion, low porosity, and high corrosion resistance [1-3]. Specifically, the TWAS process has favoured in many industries due to its low cost, simple operation condition, and high spray rate [2-4].

TWAS comprises a standard process mechanism of a thermal spray technique as illustrated in Figure 1.

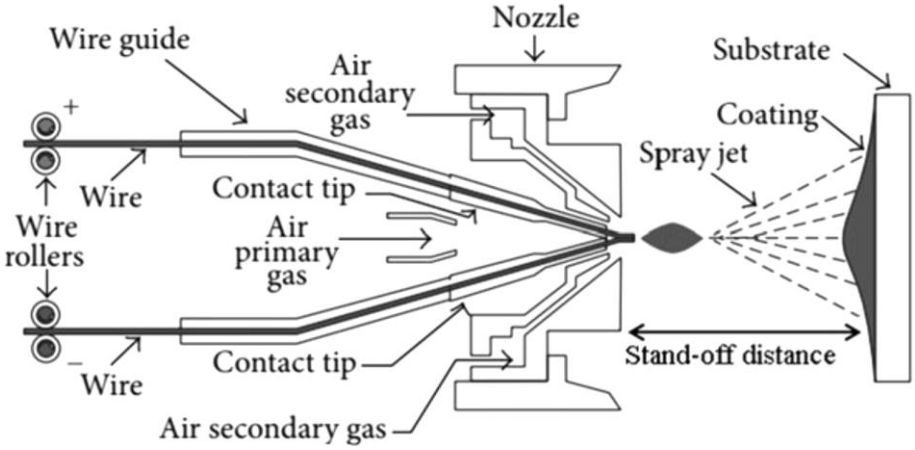

Figure 1. Illustration of TWAS process [2]

A spray torch is applied, which electrically energizes two wires feedstock together and forms an arc-like welding arc. The wires then melt, and a gas stream atomizes the molten particle and strongly propels it downstream [5]. The molten droplets flatten as they hit the substrates before solidification occurs and then form a coating by accumulating incoming particles layer by layer [6-8]. The coating will undergo significant changes concerning mechanical properties during deposition, as thermal stress buildup during impact and solidification. The formation of unwanted phases would also alter the coating's mechanical properties. Thus, the microstructural features of coating highly affect the mechanical properties of thermal spray coatings.

A decent quality coating is determined by its microstructure, phases, wear rate, corrosion resistance, oxide content, wear rate, deposition efficiency, and significant mechanical properties such as porosity, hardness, toughness, bond strength, surface roughness [8]. TWAS process has stochastic parameters including current, stand-off distance (SOD), voltage, and pressure, which substantially affect coating outcomes. Theoretically, TWAS has produced high porosity, surface roughness, and oxide content compared to other techniques despite being widely used in many industries [9-11]. Thus, it is critical to optimize

the process parameters to achieve high-quality coatings, resulting in a more extended service period.

Numerous studies have reported the effects of spray distance on coating microstructure and mechanical properties. A study on Zn coating on carbon steel via cold spray process has been performed by Djerourou et al. where they recorded that spray distance has significant effects on corrosion resistance and coating microstructure [12]. The coating prepared at 100 mm (closest spray distance) presents higher hardness and low porosity fraction than other prepared coatings. Another study conducted by Widaya et al. where they coated FeCrBSiNbW on AISI304SS through the TWAS process and varied the gun spray distance. Results have shown that shorter distances produced high wear resistance coating [13]. It is due to shorter length having a higher impact on substrate upon deposition, hence better coating consistency [14-16]. From the literature, the maximum spray distance was set at 350 mm where the coating was observed to have high porosity and low adhesion due to inconsistency during coating and lower particle speed during impact compact to shorter distances [17].

Different materials have been used as wire feedstock following different applications and purposes. Aforementioned, metallization is an effective way to improve the corrosion resistance of steel [10] and among the most commonly used metals for such purposes are aluminium (Al), zinc (Zn), and its alloys. These metallic coatings act as a sacrificial anode and supply cathodic protection (CP) to the substrate. When Al/Zn coating is applied on mild steel and exposed to the marine environment, a galvanic couple is formed, this causes electrons to flow from the coating (anode) towards the substrate (cathode), leading to the dissolution of the coating while the substrate is protected [18]. Due to their excellent properties, extensive research on Al and Zn alloys coatings have been conducted for years as Al alloys coatings are proven to protect components effectively in many industries. Another reason for the high demand for Al and Zn coatings on mild steel is because they are more economical and offer double protection from corrosion. At the same time, Zn coating offers CP, Al coating functions as a barrier by forming a thin oxide layer [19-20].

A pseudo-alloy coating is formed when two different wire feedstocks are sprayed simultaneously, e.g., Al and Zn wired are combined to form Al-Zn coating, which comprises the quality of both elements; physio-chemical and mechanical properties of the deposited materials. Previous studies have reported that the performance of AlZn pseudo-alloy coating with the composition 55Al-45Zn was much better than 15Al-85Zn, pure Zn and Al coatings in terms of corrosion [16-17].

However, to the best of the author's knowledge, limited studies have been performed to study the effects of different parameters of the TWAS process on Al-Zn pseudo-alloy coating properties. Therefore, in this study, the properties of AlZn pseudo-alloy coating developed using TWAS were investigated to study the effect of stand-off parameters on coating quality.

Materials and Methods

Feedstock and substrate material. In this research, two sprayed materials, from Sulzer-Metco Inc. were utilised: (a) Al wire (99.5%), and (b) Zn wire (99.9%). Both were 1.6 mm in diameter to produce an Al-Zn pseudo-alloy coating that imitated Al-50Zn composition

by controlling the feed rate of both inputs using a robot arm and robotic system to obtain a homogeneous coating thickness. Wires were deposited on mild steel substrates (150 x 50 x 3 mm) with the composition tabulated in Table 1.

Table 1. Mild steel substrates chemical composition.

Element	Fe	C	Al	Mn	P	Si	S
Percentage (wt.%)	Balance	0.04	0.03	0.2	0.03	0.01	0.004

Substrate preparation and coating process. Pre-treatment using sandblasting NORBLAST machine by Norexo were conducted on substrates at room temperature, 4 bar pressure, 45° attack angle before the coating process to clean dirt, dust, and enhance the adhesion through mechanical interlocking mechanisms. After the grit-blasting process, the samples were cleaned with acetone and dried using an air dryer. The average surface roughness valued at 75–100 μm were obtained following SA3 (ISO 8503) [16] surface profile quality standards by NACE. An automatic arc spray gun type ARCSPRAY, also from Sulzer-Metco Inc. connected to a DC power supply, was used to produce Al-50Zn coating. The process parameters are summarized in Table 2.

Table 2. Coating process parameters and SOD values

Spray Parameters	Value
Air pressure	3.0 bar
Current spraying	150 A
Voltage spraying	30 V
Substrate temperature	Room temperature
Feed wire materials	99.5% Al and 99.9% Zn
Wire size of Al and Zn	1.6 mm diameter
Stand-off distance (SOD)	100, 150, 200, 250, 300 mm
Coating duration (s)	15 - 20

The gun distance applied from substrates were varied from 100 mm to 300 mm. Other parameters were set at a constant rate such as compressed air pressure at 3 bar and spray angle at 90°. The current and voltage were also kept at a constant rate following previous studies [21] to focus on the effect of SOD on coating quality. All coated samples were analysed to study their morphology and properties concerning different values of SOD.

Coating characterization. The microstructure of the Al-50Zn coating surface at random locations and its cross-section were analysed using a scanning electron microscope (SEM model JEOL JSM-6360LV). Samples were sectioned, mounted in epoxy (Buehler trans-optic powder) and subjected to 1200 grit grinding. Then, polishing was performed using 3-micron diamond suspension on Spec-Cloth to ensure it was suitable for metallography analysis. This was performed to better understand the distribution of porosity and splat formation and accurately measure coating thickness. Image software (ImageJ v. 1.47) was utilised to analyse SEM images and compute the mean porosity using the images captured (ASTM E2109-01) [22-23].

X-ray diffraction (XRD, Bruker D8 Advance model USA) in the range of 2θ = 10 - 90° was used to analyse the crystal structure and phases of coating, and quantitative analysis of phases composition. The spectrum was compared with a standard database of JCPDS.

Samples were cured and mounted in epoxy, polished with diamond pastes to enhance surface quality.

In addition to the cross-sectioned thickness analysis, a nondestructive gauge was also utilized for coating thickness by measurements were taken at five different locations and the average was recorded. Vickers indentation was performed on the coating surface and cross section, at random locations where 1 kgf load was applied for 15 s (ASTM E384-17) [21]. Ten indentations were made for higher accuracy results.

A pull-off test was conducted to investigate the adhesion properties of deposited coating to mild steel substrates in 12 cm^2 following the standard (ASTM C633-13) using Elcometer 634. Samples were adhered to a non-sprayed counterpart. Meanwhile, the surface roughness (R_a) was determined using a profilometer (SJ-210 Mitutoyo) with a resolution of 0.05 μm and maximum measuring range of 10 μm. Ten different measurements of each sample were taken randomly to minimize errors. It is worth mentioning that the location chosen for all tests might have affected coating properties analysis due to unwanted phases. Therefore, testing was conducted at random places on sample for accuracy and consistency.

Results and Discussion

Morphology and microstructure. The lamellar structure is typical for an arc spray coating [22] and was captured in this study using SEM. From the analysis, the material deposited was generally very homogeneous and compact for a coating via wire arc spray technique. It was found that the microstructure of the coating sample prepared at 100 mm SOD to be denser with fine grains compared to others, and this was also supported by the hardness test results in Figure 6. The effect of SOD on coating microstructure is related to the amount of unmelted coating material and porosity. An increase in SOD produced results in unmelted particles and higher porosity as higher SOD leads to a lower temperature of in-flight particle before hitting the substrate, hence less consistency during impact [5]. The best coating properties with the lowest porosity were achieved at SOD of 100 mm instead of 300 mm where a lot of deposition inconsistency was formed.

Coatings prepared at 100 mm were denser with refined grains microstructure compared to the coating deposited at parameters 150 mm and 200 mm SOD respectively. Image analysis on the cross section was performed to determine the microstructure, porosity fraction, and thickness of the coating are shown in Figure 2.

From SEM analysis images, coating thickness increased proportionally to SOD value, where coating deposited at 300 mm SOD developed the highest thickness compared to 100 mm SOD, as shown in Figure 3.

The mean porosity distribution value was computed using ImageJ software by adjusting the brightness and contrast to achieve grey and dark region where the dark area represented the porosity. An example of surface morphology of coating material by SEM with 4000×magnification, where porosity, unmelt material, and oxide have appeared as shown in Figure 4.

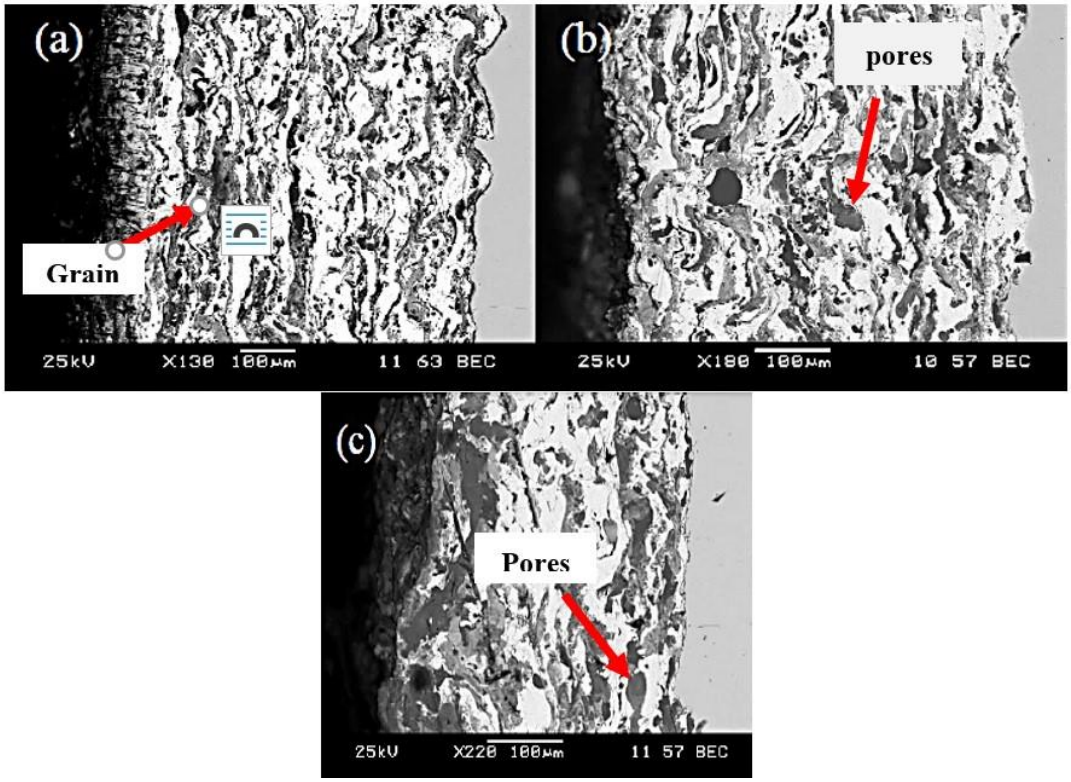

Figure 2. SEM images of arc TWAS Al-50Zn coating at different SOD (a) 100 mm, (b) 150 mm and (c) 200 mm.

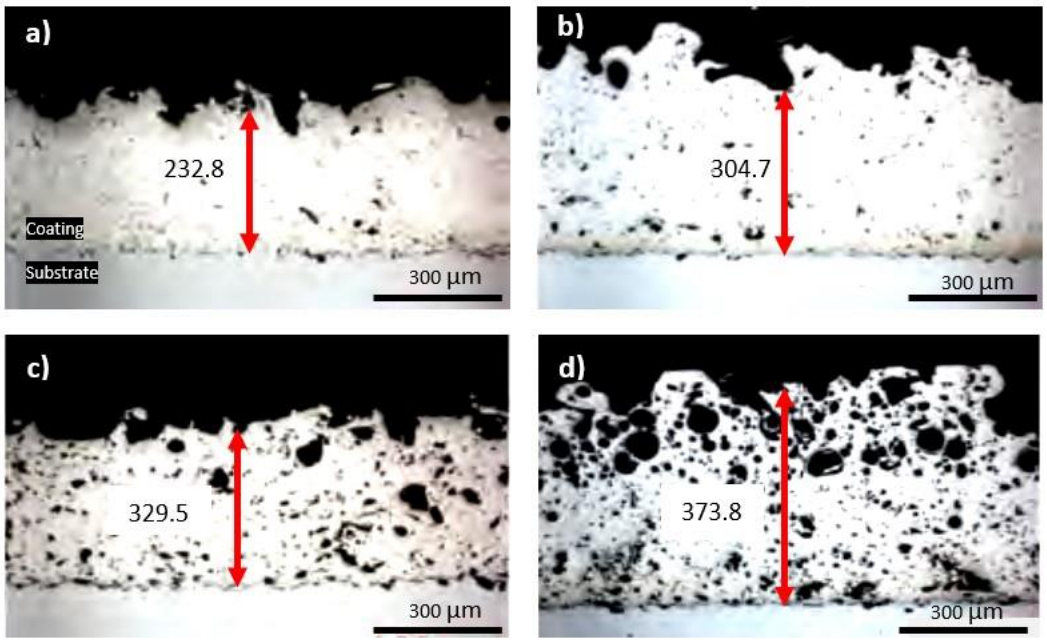

Figure 3. Cross-section images of Al-50Zn coating displaying porosity and thickness value at different SOD a) 100 mm, b) 150 mm, c) 250 mm, and d) 300 mm.

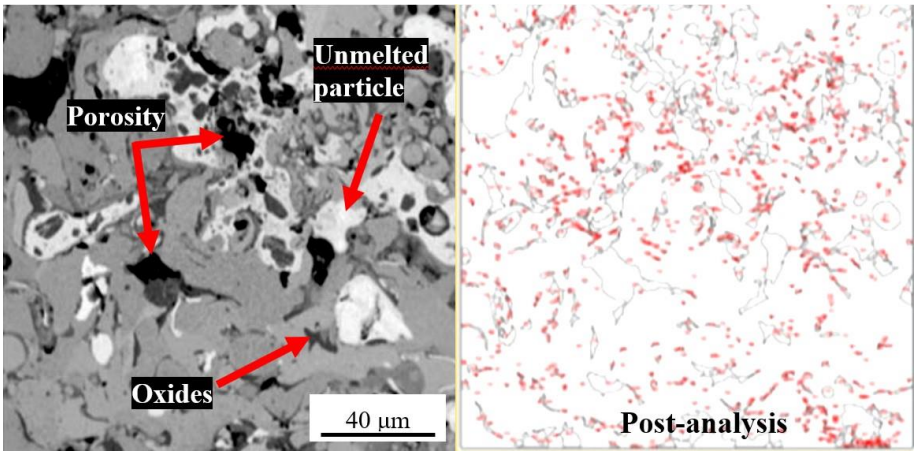

Figure 4. A micrograph for porosity distribution analysis for coating sample at 100 mm SOD using ImageJ software.

The results have depicted that porous deposit was formed by unmelted particles, splat boundaries, melted clusters, and differences in the chemical composition of Al and Zn. A porosity average of 5.13 – 9.73% range was obtained from the analysis where coating at 100 mm SOD had the lowest value. It is important to note that the total measured porosity distribution was also affected by cracks, voids, splat boundaries, and some undetected oxide phases.

This method has been performed by Lin et al. previously where similar results were obtained [24]. From the images in Figure 3, it could be observed that there was a correlation between porosity and coating hardness as discussed in the next section where porosity fraction was directly opposite to hardness values. As SOD was shifted from 100 mm to 300 mm, SEM images were examined and have shown an increasing trend in porosity fraction value, thus decreasing the hardness.

The results obtained are similar to previous studies as higher SOD leads to a longer time in the air for the molten particles before reaching the substrates; thus, oxidation takes place at a higher rate [23-25]. Subsequently, the coating contained more defects such as oxides inclusion and partially molten particles causing higher porosity distribution, which explains the higher density obtained at 100 mm SOD with a lower porosity fraction.

Energy-dispersive X-ray spectroscopy (EDS) analysis was performed at random locations in the gray area to investigate the elemental composition of coating quantitatively. Overall analysis has confirmed the formation of a pseudo-alloy coating with a composition of Al50-Zn50 mainly composed of Al, Zn, and O with some impurities such as iron and copper, as indicated in Table 3.

Table 3. wt.% of Al-Zn coating.

Compound	wt.%
Al	51.07
Zn	43.21
O	1.72

The wt.% is reasonable and consistent with the coating process objective given the use of an automatic robot arm. Trace of oxygen indicated the presence of oxidation in the form of a crystalline aluminium oxide layer. It was thought to act as a protective layer protecting the substrate against corrosion.

EDS analysis has revealed that the sprayed arc particles were oxidized during the coating process. In the TWAS technique, the oxidation of molten particles causes high oxide content. Therefore, it can be speculated that the amount of oxides in the coating increases relative to higher SOD. During spraying, the longer time for molten particles in the air before hitting the substrates causes such significant in-flight oxidation. However, this needs further investigation [24-25].

XRD analysis was conducted to investigate the crystal structure and coating phases. According to the Al-Zn phase diagram, the results have revealed that, two principal phases were observed for all prepared coating at different SOD as shown in Figure 5.

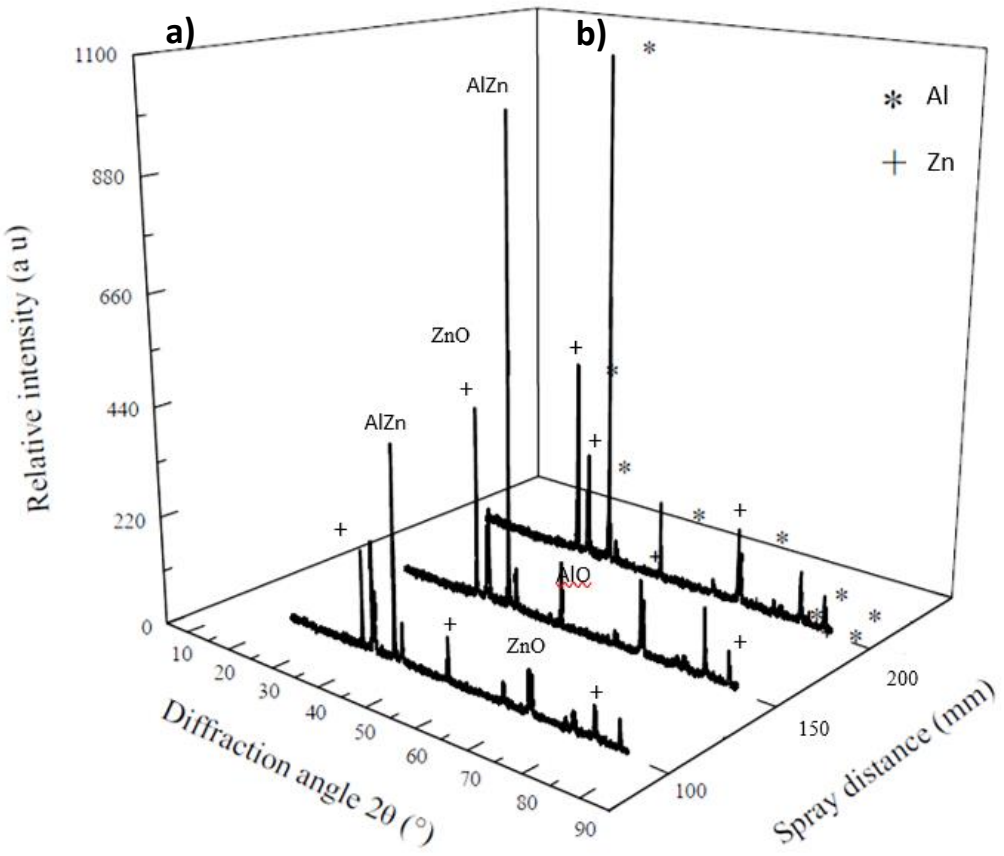

Figure 5. XRD spectra of Al-50Zn coating at different SOD (100 mm, 150 mm, 200 mm)

It was observed that the coating was mainly composed of three elements: Al, Zn, and O (Al-Zn), aluminum oxide (AlO) and zinc oxide (ZnO). The aluminium-rich phase provided protection and barrier action from the formation of the oxide layer, while zinc-rich phase known for its sacrificial coating offers cathodic protection. It was observed that the peak intensity of the different phases increased when the spray distances increased. This could be due to the higher crystallinity of oxide as SOD increased. The kinetics of AlO coatings is interface-controlled and largely dependent on the applied current density. Al-Zn peak was

observed on the coating at 150 mm SOD where traces of ZnO and AlO were present in all coating samples which could protect the substrates.

Mechanical properties of the coating. As stated before, the heterogeneous microstructure of coating in TWAS highly influences its mechanical properties, resulting in complex and anisotropic mechanical properties The aim of this research was to characterize the mechanical properties of Al-50Zn coating prepared via the TWAS process. Comparing the microstructural and phases analysis with its mechanical properties is vital to investigate the relationship of all features.

Aforementioned, coating thickness was also measured using a nondestructive gauge to validate the measurements from SEM analysis. The spray gun was initially set at 100 mm away from substrates and then increased every 50 mm until 300 mm to get apparent differences. A trend of increase was observed where higher SOD produced higher coating thickness. The highest SOD at 300 mm was found to have the highest thickness as coating materials particles scattered wider, thus, inconsistent coverage and lesser impact on substrates. In contrast, coating deposited at 100 mm SOD have the lowest thickness with an average of 217 μm, which falls in the standard range for Al coating performed via TWAS [18]. Thickness values with respect to SOD are shown in Table 4.

Table 4. Coating thickness at different SOD.

Stand-off distance (mm)	Coating thickness avg (μm)	Standard deviation
100	217	11.21
150	285	11.54
200	324	10.24
250	371	10.98
300	416	12.41

An average increment of 75% in coating thickness from the sample at 100 mm SOD to 300 mm was calculated from the results. As investigated by previous studies, the thickness increased with SOD range from 100 mm to 300 mm where higher thickness led to lower adhesion and hardness. This could be observed from porosity distribution from SEM images in Figure 3, where coating at higher SOD had higher porosity. This is supported by an adhesion test where the bond strength coating at 100 mm was found to be the highest due to better deposition of particles impact on substrates. Higher SOD produced lower adhesion. The highest adhesion value was found in the sample with the lowest SOD at 8.3 MPa, while 300 mm SOD recorded an average of 6.22 MPa as shown in Figure 6.

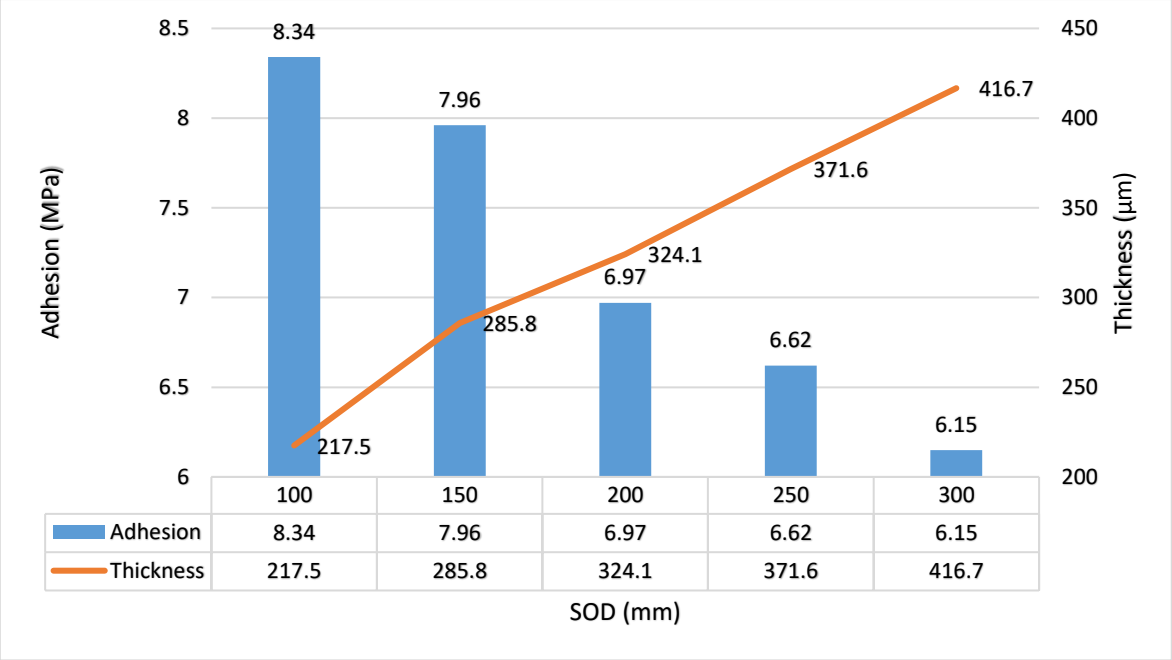

Figure 6. Coating thickness and adhesion at different SOD

Coating parameters also affected the microhardness significantly and its porosity properties, as discussed previously. An increase in SOD resulted in high porosity thus a lower hardness value of the deposited layer as seen under the microscope. From the hardness test of 10 indentations, the uncoated substrate surface had a hardness value of 43.29 HV, whereas the coated surface had a hardness range of 60 – 110 HV. Except for 300 mm, all coating hardness has achieved the minimum hardness criteria on impeller after coating. Following the literature, higher coating thickness was found to have lower hardness after testing using Vickers microhardness. It could be because of better deposition occurs at lower SOD where more uniform structure and less thermal stress buildup were observed. The highest hardness value, 167.33 HV has appeared in the sample with has a SOD of 100 mm as shown in Figure 7.

TWAS coating usually produces an inhomogeneous surface profile compared to other coating techniques, which can be seen from roughness test results. It was observed that the surface roughness increased as SOD increased where SOD at 100 mm recorded R_a = 5.132 microns in contrast to 300 mm SOD with the highest roughness, around 27% increment. High SOD resulted in high surface roughness. This trend was observed because longer SOD is associated with slower particle speed upon impact on substrates, causing inconsistency and higher splat boundaries. Shorter SOD produces smaller particle sizes deposition on substrates thus resulting in higher density and hardness value with smoother surface roughness [13]. The roughness values at different SOD are summarized in Table 5.

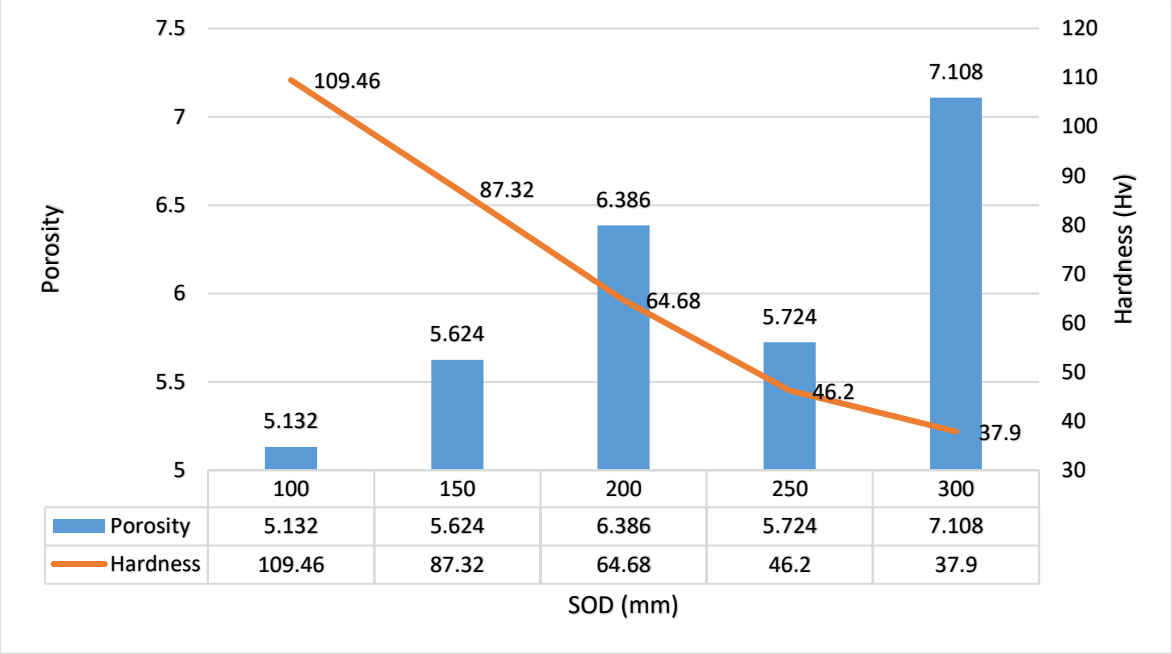

Figure 7. Coating hardness and porosity at different SOD

Table 5. Coating surface roughness at different SOD

SOD (mm)	Surface roughness (microns)	Standard deviation (SD)
100	5.132	13.54
150	5.624	17.36
200	5.686	15.21
250	5.724	19.26
300	6.508	17.13

Drastic temperature loss causes significant delamination of sprayed particles, yielding a rougher surface. The consistency of coating material during impact is directly tied to gun spray distance, such lower SOD produces a denser coating with lower porosity, smoother surface roughness, high hardness, and high adhesion. Overall, SOD at 100 mm produced the most optimum coating quality.

Conclusion

Al-50Zn pseudo alloy coating was successfully deposited via TWAS, with varied spray distances. However, results have indicated some defects and high porosity for coating at higher SOD. This could be caused by unmelted in-flight particles and splat boundaries during impact. Cross-section images of coating porosity distribution have been observed by SEM analysis where higher SOD resulted in higher porosity and thickness. The microstructure of coating deposition at 100 mm SOD also has shown a consistent lamellar structure compared to others. Lower SOD is believed to produce better coating quality including adhesion, hardness, lower porosity, and lower surface roughness as achieved in deposition coated at 100 mm SOD where adhesion was 8.9 MPa and roughness at 5.1 microns.

Acknowledgements

This study was financially supported by UTM Zamalah Scholarship and TDR Grant Scheme Vot No. 06G22.

Author Contributions

All authors contributed toward data analysis, drafting and critically revising the paper and agree to be accountable for all aspects of the work.

Disclosure of Conflict of Interest

The authors have no disclosures to declare

Compliance with Ethical Standards

The work is compliant with ethical standards

References

[1] Goodwin, F.E. (2010). Corrosion of Zinc and its Alloys. *Corr. Degr. of Eng. Mat.* 3(7) 2078-2089.

[2] Bratean, L., Miclosi V., Voiculescu I. & Iacobescu G. (2011). Research on anticorrosion characteristics of AlZn pseudo-alloy obtained by metal-arc process. *Mat. Sci. Series*, 73 153-164.

[3] Kumar, D., Murtaza, Q. & Singh, R.C. (2015). Sliding wear behavior of aluminium alloy coating prepared by two-wire electric arc spray process. *Int. J. Adv. Man. Tech.* 170(15) 7920-7936.

[4] Bratean L. (2015). Thermal spraying arc process with two dissimilar wires – quality tests. In Procedia – *Social and Behavioral Sciences,* 180(10) 1116-1124.

[5] Syrek, G. B., Paul, S. & Davenport, A.J. (2020). Sacrificial thermally sprayed aluminium coatings for marine environments. *A rev., MDPI coat.* 10 267-274.

[6] Esfahani, E.A., Salimaji, H., Golozar, M.A., Mostaghimi, J. & Pershin, L. (2012). Study on corrosion behavior of arc sprayed aluminum coating on mid steel. *J. Therm. Spr. Tech.* 21(6) 1195-1202.

[7] Brito, V.R.S., Bastos, I.N. & Costa. (2012). Corrosion resistance and characterization of metallic coatings deposited by thermal spray on carbon steel. *Mat. and Des.* 41 282-288.

[8] Seung, L. H., Singh, J.K., Ismail, M.A., Bhattacharya, C., Seikh, A.H., Alharthi, N. & Hussain, R.R. (2019). Corrosion mechanism and kinetics of Al-Zn coating deposited by arc thermal spraying process in saline solution. *Nature Sci. Rep. J.* 9 3399-3416.

[9] Chungsheng, M., Juan, L., Xinhe, Z., Wenbin, X., Zhijun, Y., Dong, C., Jingguo, F. & Shenglin, M. (2020). Anticorrosive non-crystalline coating prepared by plasma electrolytic oxidation for ship low carbon steel pipes. *Scien. Rep. Nature Res.* 10 1567-1574.

[10] Liu, R. (2014). Discharge behaviors during plasma electrolytic oxidation on aluminum alloy. *Mater. Chem. Phys.*, 148 284-293.

[11] Amir, D. & Fardad, A. (2020). Investigation on Relationship Between Microstructural Characteristics and Mechanical Properties of Wire-Arc-Sprayed Zn-Al Coating. *J Therm. Spray Tech*. 29 297 – 307.

[12] Djerourou, K., Hernas, A., Moskal, G. & Myalska H. (2015). Thermally Sprayed Coatings Resistant to Erosion and Corrosion for Power Plant Boilers—A Review. *Surf. Coat. Tech.* 268 153-167.

[13] Fitriyana, D.F., Caesarendra, W., Nugroho, S., Haryadi, G.G., Herawan, M.A., Rizal, M. & Ismail, R. (2019). The effect of stand-off distance on the twin wire arc spray (TWAS) coating for pump impeller from AISI 304SS. *Springer Pro. in Phys.* 242(4) 119-128.

[14] Khlusova, E. I. & Orlov, V. V. (2013). Change in the structure and properties in the heat affected zone of welded joints made from low carbon ship-building and pipe steels. *Met.* 56 684-697.

[15] Yang, W., Liu, W., Peng, Z., Liu, B. & Liang, J. (2017). Characterization of plasma electrolytic oxidation coating on low carbon steel prepared from silicate electrolyte with Al nanoparticles. *Cer. Inter.* 43 16851-16863.

[16] Ma, C. (2019). Influence of microarc oxidation power supply frequency on tribology performance of a self-lubricating coating for Al–Si diesel engine pistons. *Mater. Res. Exp.* 6 1165-1173.

[17] Wang, Y. & Jiang, Z. (2009). In situ formation of low friction ceramic coatings on carbon steel by plasma electrolytic oxidation in two types of electrolytes. *App. Surf. Sci.* 255 6240-6251.

[18] Wang, Y., Jiang, Z. & Yao, Z. (2009). Microstructure, bonding strength and thermal shock resistance of ceramic coatings on steels prepared by plasma electrolytic oxidation. *App. Surf. Sci.* 256 650–656.

[19] Chen, Z. & Xia, Y. A. (2011). The crack propagating behavior of composite coatings prepared by PEO on aluminized steel during in situ tensile processing. *Mat. Sci Eng. A Stru.* 528 1409-1421.

[20] Moridi, A., Hassani-Gangaraj, S. M., Guagliano M. & Dao M. (2014). Cold Spray Coating: Review of Material Systems and Future Perspectives. *Surf. Eng.* 30(6) 369-382.

[21] Swaminathan, V., Zeng, H., Lawrynowicz,, D, Zhang Z. & Gilbert, J.L. (2012). Electrochemical Investigation of Chromium Nanocarbide Coated Ti-6Al-4V and Co-Cr-Mo Alloy Substrates. *Electrochim. Acta*, 59 387-399.

[22] Folkeson, N., Jonsson, T., Halvarsson, M., Johansson, L. G. & Svensson, J.E. (2011). The Influence of Small Amounts of KCl(s) on the High Temperature Corrosion of a Fe-2.25Cr-1Mo Steel at 400 and 500 C. *Mat. Corr.* 62 606-617.

[23] Ehlers, J. (2006). Enhanced Oxidation of the 9%Cr Steel P91 in Water Vapour Containing Environments. *Corr. Sci.* 48(11) 3428-3435.

[24] Fauchais, B. & Vardelle A. (2012). Thermal Sprayed Coatings Used Against Corrosion and Corrosive Wear. *Adv. Plasma Spr. App.* 55 2312-2323.

[25] Lin, J., Wang, Z., Lin, P., Cheng, J., Zhang, X. & Hong, S. (2015). Effects of post annealing on the microstructure, mechanical properties and cavitation erosion behavior of arc-sprayed FeNiCrBSiNbW coatings. *Mat. Des.* 65 1035–1040.